J|A|C|S
COMMUNICATIONS

Published on Web 02/13/2004

Interrogating Conformationally Dependent Electron-Transfer Dynamics via Ultrafast Visible Pump/IR Probe Spectroscopy

Igor V. Rubtsov, Naomi P. Redmore, Robin M. Hochstrasser,* and Michael J. Therien*
Department of Chemistry, University of Pennsylvania, Philadelphia, Pennsylvania 19104-6323
Received September 23, 2003; E-mail: therien@sas.upenn.edu

It has long been recognized that the magnitude of donor−acceptor (D−A) electronic coupling could depend sensitively upon both D−A orientation and the overall conformation of donor−spacer−acceptor (D-Sp-A) assemblies.[1] For D-Sp-A systems that manifest a high degree of ground-state structural heterogeneneity, where simple theoretical analyses predict a wide distribution of configurationally dependent electron transfer (ET) rate constants, such conformational and orientational control of ET dynamics has been little studied.[2] In this report, we demonstrate for the first time the utility of the time-resolved visible pump/mid-infrared (IR) probe spectroscopy[3] to interrogate directly, and provide unique information regarding, conformationally dependent photoinduced ET dynamics and the subsequent structural evolution of the resulting charge-separated state.

The particular efficacy of ultrafast IR spectroscopy in the investigation of ET processes derives from the fact that IR vibrational bands are narrow: vibrational frequencies are thus sensitive to molecular electronic states and therefore enable state-specific detection. Furthermore, because vibrational transitions are more spatially localized than electronic transitions, transient IR spectra inherently possess considerable structural information. Fast visible pump/IR probe methods consequently merge the advantages of vibrational spectroscopy (spectral resolution and sensitivity) with the time resolution provided by short fs laser pulses. Exemplary visible pump/IR probe experiments involving *N*-[5-(10,20-diphenylporphinato)zinc(II)]-*N*′(octyl)pyromellitic diimide (**PZn−PI**) and [5-[4′-(*N*-(*N*′-octyl)pyromellitic diimide)phenyl)ethynyl]-10,20-diphenylporphinato]zinc(II) (**PZn()PI**) (Figure 1) emphasize these points.

The photoinduced charge separation (CS) and thermal charge recombination (CR) ET dynamics of **PZn−PI** and **PZn()PI** have been characterized previously using visible pump−probe spectroscopy;[4] in these systems, $k_{CS} \gg k_{CR}$ for **PZn−PI**, while the opposite is true for **PZn()PI** [mean rate constants: **PZn−PI** $k_{CS} = 1.9$ ps^{-1}, $k_{CR} = 15$ ps^{-1}; **PZn()PI**: $k_{CS} = 22$ ps^{-1}, $k_{CR} = 3.3$ ps^{-1} (99:1 $CDCl_3$:pyridine; 23 °C)]. Figure 1A exhibits the IR fingerprint of the S_1-excited state of a benchmark (porphinato)zinc(II) (**PZn**) complex, ([5,10,15,20-tetraphenylporphinato]zinc(II), **TPPZn**) obtained 1 ps following electronic excitation, while Figure 1B shows the polarized, visible pump/IR probe transient spectra obtained for **PZn−PI** at a time delay (t_{delay}) of 0.7 ps; note that the spectrum is dominated by ground-state bleaching bands (1775, 1730, and 1375 cm^{-1}) and absorptive transitions (1655, 1440, 1300−1350 cm^{-1}) associated with the **PZn**$^+$**−PI**$^-$ CS state.[5] It is important to underscore the two intense carbonyl modes observed in the **PZn−PI** linear-IR spectrum: a strong, B-polarized transition at 1730 cm^{-1}, and a weaker A-polarized mode at 1775 cm^{-1}. These polarized vibrational modes, coupled with removal of degeneracy of the **PZn** Q_x and Q_y transitions, provide the necessary spectroscopic handles (Figure 1B) to assess the mean interplanar torsional angle between the D and A units. Previous work establishes that introduction of sufficient electronic asymmetry converts the classic **PZn** circular absorber into a C_2-symmetric elliptical chromophore,

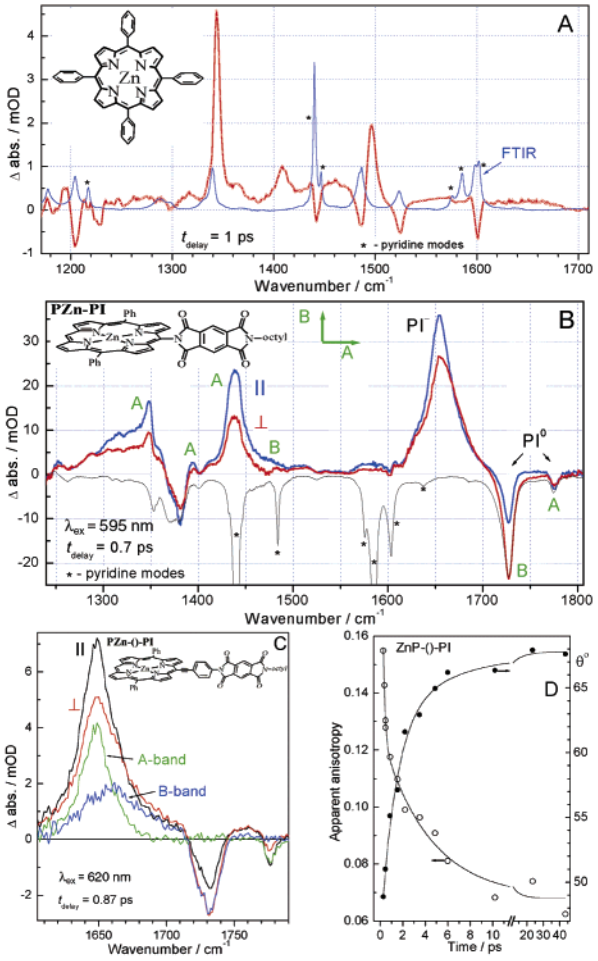

Figure 1. (A) Transient IR spectra of the **TPPZn** S_1-excited state; the FTIR spectrum is displayed for comparison. (B) Exemplary polarized visible pump/IR probe transient spectra of **PZn−PI** (FTIR spectrum, inverted). (C) Polarized transient IR spectra of **PZn()PI** with deconvoluted A- and B-polarized absorptive components highlighted. (D) Time-dependent apparent anisotropy of the **PZn**$^+$**()PI**$^-$ 1648 cm^{-1} radical anion absorption band and the corresponding **PZn−PI** torsion angle θ; the lines denote the best biexponential function fits of these respective decays (r: 180 ± 70 fs, 4.3 ± 0.8 ps; θ: 1.4 ± 0.6 ps, 7 ± 5 ps). Data were obtained at 23 ± 1 °C; other experimental conditions are indicated in the figure panel insets.

where *x*- and *y*-polarized transitions are not degenerate.[6,7] In a polarized visible pump/IR probe experiment, note that the anisotropy of the **PI** B-polarized transitions (r_B) depends on the **PZn**-to-**PI** torsional angle θ (Scheme 1), while the anisotropy of the A-polarized bands (r_A) does not. Therefore, the A-polarized band anisotropy can be related to the porphyrin Q-transition ellipticity parameter (eq 1),[7]

$$\gamma = \frac{0.2 + r_A}{0.4 - r_A} \qquad (1)$$

10.1021/ja0305499 CCC: $27.50

Scheme 1

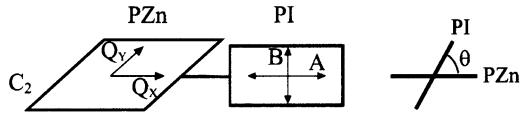

Table 1. Anisotropy Values of the IR Bleach Bands and Evaluated Ground-State Mean Interplanar Torsional Angles

	$r_A^{IR\,a}$	$r_B^{IR\,a}$	$\tilde{\theta}$ (deg)	t_{delay} (ps)
PZn−PI	0.19	−0.19	78 ± 4[b]	0.5
PZn()PI	0.18	−0.11	50 ± 3	0.47

[a] The anisotropy error is ±0.01 and ±0.005 for A and B bands, respectively. [b] See ref 8.

which describes the ratio of the *x*- and *y*-polarized S_1-state extinction coefficients at the excitation wavelength ($\gamma = \epsilon_{Qx}/\epsilon_{Qy}$); this parameter can be determined directly from the early time anisotropies. Knowing γ enables the evaluation of $\overline{\cos^2\theta}$ from the anisotropy of the B-polarized bands (eq 2):

$$\overline{\cos^2\theta} = \frac{5r_B + 1}{2 - 5r_A} \tag{2}$$

Table 1 summarizes the results of such an analysis for **PZn−PI** and **PZn()PI** at ∼0.5 ps delay times. Given the mathematical meaning of $\tilde{\theta} = \cos^{-1}\sqrt{\overline{\cos^2\theta}}$,[8] and coupling this information with electronic structural studies and MOPAC-determined dihedral angle energy distribution data,[4a,b] suggests that the mean **PZn**-to-**PI** interplanar torsional angle for electronically excited **PZn−PI** species (**^{1}PZn*−PI**) that have undergone ET at this delay time is centered at 90° with a distribution width of 14°, while the analogous angle for **^{1}PZn*()PI** at $t_{delay} = 0.5$ ps is centered at 50°.

For the inhomogeneously broadened carbonyl IR bands of Figure 1, the frequency distribution maps the torsional angle conformational distribution; the time evolution of the transient spectra can be used to monitor the ET rate dependence upon θ (Scheme 1). In this regard, the **PZn()PI** spectral evolution shows that absorption maximum of the **PI**$^-$ band at ∼1650 cm^{-1} both red-shifts 3.5 cm^{-1} and exhibits apparent anisotropy changes characterized by a 4-ps time constant (Figure 1C,D), while the anisotropy of the A-polarized bleach band at 1775 cm^{-1} decays only on the rotational time scale ($\tau_{decay} \approx 250$ ps). Note that analysis of the B-bleach band dynamics at ∼1730 cm^{-1} is complicated due to nonlinear signal contributions that derive from vibrational coupling;[9,10] such features are clear in transient spectra at later times (Figure S2). The time evolution of the transient spectra in the **PI**$^-$ absorption region (1620−1700 cm^{-1}) was therefore utilized to obtain dynamics-correlated structural information.

As $k_{CS} \ll k_{CR}$ in **PZn()PI**, the observed time evolution of the IR spectra monitors structural evolution in the **^{1}PZn*()PI** excited state: at each t_{delay}, the CS state absorption band reflects the weighted distribution of **^{1}PZn*()PI** conformers that undergo ET at that time. The measured time-dependent anisotropy and maximal absorption band frequency therefore vary with the depletion of **^{1}PZn*()PI** conformeric populations that differ with respect to torsional angle θ and necessarily manifest different CS rate constants. To evaluate the time dependence of $\tilde{\theta}$, the B-polarized vibrational mode contribution to the ∼1650 cm^{-1} band was analyzed (Figure 1C) as a function of delay time, assuming constant anisotropy of the A-polarized mode and time independence of the relative oscillator strengths of the A- and B-polarized absorptions. This analysis (Figure 1D) indicates that more planar **^{1}PZn*()PI** conformers exhibit larger-magnitude CS rate constants and that the CS states of conformers possessing larger values of $\tilde{\theta}$ dominate the observed spectrum at later times. The fast decay component suggests that there is extremely rapid depopulation of CS-state structures that feature the most extensive conjugation (∼180 fs). These data show that as electronically excited **^{1}PZn*()PI** conformers with increasingly larger average **PZn**-to-**PI** interplanar torsional angles are depopulated with time, the **PZn$^+$()PI$^-$ PZn**-to-**PI** $\tilde{\theta}$ value evolves from 49 to 67° over a 40-ps time domain. While similar dynamics are evident for **PZn−PI**, discrimination of the disparate torsional angle-dependent ET dynamics is more difficult as the mean angle θ is close to 90° and k_{CS} is of larger magnitude.[10]

In summary, we have assessed the mean **PZn**-to-**PI** interplanar torsional angle of electronically excited structural conformers that undergo ET within the sub-ps time domain for both **PZn−PI** and **PZn()PI** and have determined for the case of **PZn()PI** how this angle evolves with time. Finally, because vibrational transition moments are often known and typically localized, this work underscores that polarized visible pump/IR probe spectroscopy defines a valuable tool to interrogate structures in both electronically excited and CS states; this fact, coupled with the ultrafast time resolution and high sensitivity, makes the technique ideally suited to probe a range of mechanistic issues relevant to charge-transfer reactions.

Acknowledgment. This work was supported through the National Institutes of Health. M.J.T. thanks the Office of Naval Research (N00014-98-1-0725) and the MRSEC Program of the National Science Foundation (DMR-00-79909) for equipment grants for transient optical instrumentation.

Supporting Information Available: Details regarding experimental design and data acquisition (PDF). This material is available free of charge via the Internet at http://pubs.acs.org.

References

(1) (a) Cave, R. J.; Siders, P.; Marcus, R. A. *J. Phys. Chem.* **1986**, *90*, 1436−1444. (b) Beratan, D. N. *J. Am. Chem. Soc.* **1986**, *108*, 4321−4326. (c) Toutounji, M. M.; Ratner, M. A. *J. Phys. Chem. A* **2000**, *104*, 8566−8569.
(2) (a) Helms, A.; Heiler, D.; McLendon, G. *J. Am. Chem. Soc.* **1991**, *113*, 4325−4327. (b) Khundkar, L. R.; Perry, J. W.; Hanson, J. E.; Dervan, P. B. *J. Am. Chem. Soc.* **1994**, *116*, 9700−9709. (c) Daub, J.; Engl, R.; Kurzawa, J.; Miller, S. E.; Schneider, S.; Stockmann, A.; Wasielewski, M. R. *J. Phys. Chem. A* **2001**, *105*, 5655−5665.
(3) (a) Anfinrud, P. A.; Han, C.; Hochstrasser, R. M. *Proc. Natl. Acad. Sci. U.S.A.* **1989**, *86*, 8387−8391. (b) Okamoto, H.; Kinoshita, M. *J. Phys. Chem. A* **2002**, *106*, 3485−3490; Kumble, R.; Howard, T. D.; Cogdell, R. J.; Hochstrasser, R. M. *J. Photochem. Photobiol., A* **2001**, *142*, 121−126. (c) Heimer, T. A.; Heilweil, E. J. *Bull. Chem. Jpn.* **2002**, *75*, 899−908. (d) Marin, T. W.; Homoelle, B. J.; Spears, K. G. *J. Phys. Chem. A* **2002**, *106*, 1152−1166.
(4) (a) Redmore, N. P.; Rubtsov, I. V.; Therien, M. J. *Inorg. Chem.* **2002**, *41*, 566−570. (b) Redmore, N. P.; Rubtsov, I. V.; Therien, M. J. *J. Am. Chem. Soc.* **2003**, *125*, 2687−2696. (c) Yoshida, N.; Ishizuka, T.; Yofu, K.; Marukami, M.; Miyasaka, H.; Okada, T.; Nagata, Y.; Itaya, A.; Cho, H. S.; Kim, D.; Osuka, A. *Chem. Eur. J.* **2003**, *9*, 2854−2866.
(5) The excited-state transient IR signals of **PZn−PI** and **PZn−()-PI** are negligible relative to those of their respective CS states in the 1610−1800 cm^{-1} region.
(6) Gouterman, M. In *The Porphyrins*; Dolphin, D., Ed.; Academic Press: London, 1978; Vol. III, pp 1−165.
(7) (a) Kumble, R.; Palese, S.; Lin, V. S.-Y.; Therien, M. J.; Hochstrasser, R. M. *J. Am. Chem. Soc.* **1998**, *120*, 11489−11498. (b) Shediac, R.; Gray, M. H. B.; Uyeda, H. T.; Johnson, R. C.; Hupp, J. T.; Angiolillo, P. J.; Therien, M. J. *J. Am. Chem. Soc.* **2000**, *122*, 7017−7033. (c) Rubtsov, I. V.; Susumu, K.; Rubtsov, G. I.; Therien, M. J. *J. Am. Chem. Soc.* **2003**, *125*, 2687−2696. (d) Wynne, K.; Hochstrasser, R. M. *Chem. Phys.* **1993**, *171*, 179−188. (e) Wynne, K.; LeCours, S. M.; Galli, C.; Therien, M. J.; Hochstrasser, R. M. *J. Am. Chem. Soc.* **1995**, *117*, 3749−3753.
(8) Experimentally determined $\tilde{\theta}$ can represent a θ angle range limited by two different distribution scenarios: (i) narrow distribution around $\tilde{\theta}$ and (ii) wider distribution centered at 90° having, if Gaussian, a mean distribution width of approximately 90° $\tilde{\theta}$.
(9) Rubtsov, I. V.; Hochstrasser, R. M. *J. Phys. Chem. B* **2002**, *106*, 9165−9171.
(10) Rubtsov, I. V.; Kang, Y.; Redmore, N. P.; Therien, M. J. Manuscript in preparation.

JA0305499